Appendix A
Norms

A.1 Vector Norms

Definition A.1 *Vector norm*: A vector norm on $\mathbb{R}^n$ is a function $|| \; || : \mathbb{R}^n \to \mathbb{R}$, which fulfills the following properties:

(i) $||\boldsymbol{x}|| \geq 0$ for all $\boldsymbol{x} \in \mathbb{R}^n$
(ii) $||\boldsymbol{x}|| = 0$ iff $\boldsymbol{x} = 0$
(iii) $||\boldsymbol{x} + \boldsymbol{y}|| \leq ||\boldsymbol{x}|| + ||\boldsymbol{y}||$
(iv) $||\alpha \boldsymbol{x}|| = |\alpha| \, ||\boldsymbol{x}||$

We use the *Hölder* or *p-norms*, which are defined by

$$||\boldsymbol{x}||_p = \left(\sum_{i=1}^{n} |x_i|^p \right)^{1/p} \quad \text{with } p \geq 1 \,. \tag{A.1}$$

Therefore, we compute, e.g., the *1-norm*, *2-norm*, and ∞*-norm* as follows

$$||\boldsymbol{x}||_1 = \sum_{i=1}^{n} |x_i| \tag{A.2}$$

$$||\boldsymbol{x}||_2 = \left(\sum_{i=1}^{n} |x_i|^2 \right)^{1/2} \tag{A.3}$$

$$||\boldsymbol{x}||_\infty = \max_i |x_i| \,. \tag{A.4}$$

The *p-norms* have the following useful properties

- $|\boldsymbol{x}^T \boldsymbol{y}| \leq ||\boldsymbol{x}||_p ||\boldsymbol{y}||_q$, $\frac{1}{p} + \frac{1}{q} = 1$ (Hölder inequality)
- $|\boldsymbol{x}^T \boldsymbol{y}| \leq ||\boldsymbol{x}||_2 \, ||\boldsymbol{y}||_2$ (Cauchy–Schwarz inequality)
- $||\boldsymbol{x}||_2 \leq ||\boldsymbol{x}||_1 \leq \sqrt{n} ||\boldsymbol{x}||_2$
- $||\boldsymbol{x}||_\infty \leq ||\boldsymbol{x}||_2 \leq \sqrt{n} ||\boldsymbol{x}||_\infty$
- $||\boldsymbol{x}||_\infty \leq ||\boldsymbol{x}||_1 \leq n ||\boldsymbol{x}||_\infty$

M. Kaltenbacher, *Numerical Simulation of Mechatronic Sensors and Actuators*,
DOI 10.1007/978-3-642-40170-1

With the help of norms we can define a distance on a vector space, and furthermore, we call a vector space with a norm a normed space.

A.2 Matrix Norms

Definition A.2 *Matrix norm*: A matrix norm on $\mathbb{R}^{n \times m}$ is a function $|| \; || : \mathbb{R}^{n \times m} \rightarrow \mathbb{R}$, which fulfills the following properties:

(i) $||\boldsymbol{A}|| \geq 0$ for all $\boldsymbol{A} \in \mathbb{R}^{n \times m}$
(ii) $||\boldsymbol{A}|| = 0$ iff $\boldsymbol{A} = 0$
(iii) $||\boldsymbol{A} + \boldsymbol{B}|| \leq ||\boldsymbol{A}|| + ||\boldsymbol{B}||$ for all $\boldsymbol{A}$, $\boldsymbol{B} \in \mathbb{R}^{n \times m}$
(iv) $||\alpha \boldsymbol{A}|| = |\alpha| \, ||\boldsymbol{A}||$ for all $\alpha \in \mathbb{R}$ and $\boldsymbol{A} \in \mathbb{R}^{n \times m}$

The matrix norm associated to the vector *p-norm* is defined by the operator norm

$$||\boldsymbol{A}||_p = \sup_{\boldsymbol{x} \neq 0} \frac{||\boldsymbol{A}\boldsymbol{x}||_p}{||\boldsymbol{x}||_p} \, . \tag{A.5}$$

Other matrix norms are

$$||\boldsymbol{A}||_F = \left(\sum_{i=1}^{n} \sum_{j=1}^{m} |a_{ij}|^2 \right)^{1/2} \quad \textit{Frobenius} \text{ or } F\textit{-norm} \tag{A.6}$$

$$||\boldsymbol{A}||_1 = \max_j \sum_{i=1}^{n} |a_{ij}| \quad \text{column sum norm} \tag{A.7}$$

$$||\boldsymbol{A}||_\infty = \max_i \sum_{j=1}^{m} |a_{ij}| \quad \text{row sum norm} \, . \tag{A.8}$$

Appendix B
Scalar and Vector Fields

Definition B.1 (*Scalar field*) If we assign to each point in $\mathbb{R}^3$ defined by the vector $\boldsymbol{r}$ a scalar quantity $V(\boldsymbol{r})$ (e.g., electric potential, temperature, acoustic velocity potential), then V is called a scalar field.

For the illustration of scalar fields we use iso-lines in the 2D case and iso-surfaces in the 3D case, where the scalar quantity $V(\boldsymbol{r})$ is constant (Fig. B.1).

Definition B.2 (*Vector field*) If we assign to each point $\mathbb{R}^3$ defined by the vector $\boldsymbol{r}$ a vector quantity $\boldsymbol{F}(\boldsymbol{r})$ (e.g., electric field, magnetic field, mechanical deformation), then $\boldsymbol{F}$ is called a vector field.

Vector fields are divided into *irrotational* vector fields (e.g., electrostatic field) and *solenoidal* vector fields (e.g., magnetic field) as shown in Fig. B.2 (see also Sects. B.12 and B.13).

The lines of force (see Fig. B.3) are defined by

$$\boldsymbol{F}(\boldsymbol{r}) \times \mathrm{d}\boldsymbol{r} = \boldsymbol{0}\,, \tag{B.1}$$

which means that in each point of the lines the field vector $\boldsymbol{F}$ is parallel to the tangential vector.

In the following, we try to compute the lines of force for the vector field

$$\boldsymbol{F}(\boldsymbol{r}) = \frac{\boldsymbol{r}}{r^3} \tag{B.2}$$

with the help of (B.1). Since we are just interested in the direction, we have to solve

$$\boldsymbol{r} \times \mathrm{d}\boldsymbol{r} = \boldsymbol{0}\,. \tag{B.3}$$

By using a Cartesian coordinate system, we obtain

$$\boldsymbol{r} = x\boldsymbol{e}_x + y\boldsymbol{e}_y + z\boldsymbol{e}_z \tag{B.4}$$

$$\mathrm{d}\boldsymbol{r} = \mathrm{d}x\boldsymbol{e}_x + \mathrm{d}y\boldsymbol{e}_y + \mathrm{d}z\boldsymbol{e}_z\,, \tag{B.5}$$

M. Kaltenbacher, *Numerical Simulation of Mechatronic Sensors and Actuators*,
DOI 10.1007/978-3-642-40170-1

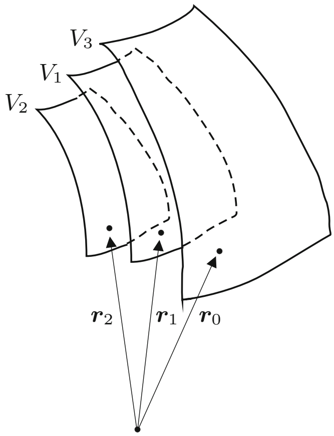

Fig. B.1 Illustration of a scalar field V with the help of equipotential surfaces

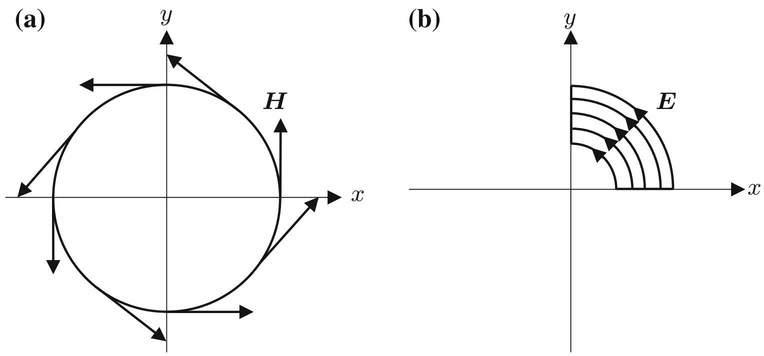

Fig. B.2 Vector fields. **a** Solenoidal vector field, **b** irrotational vector field

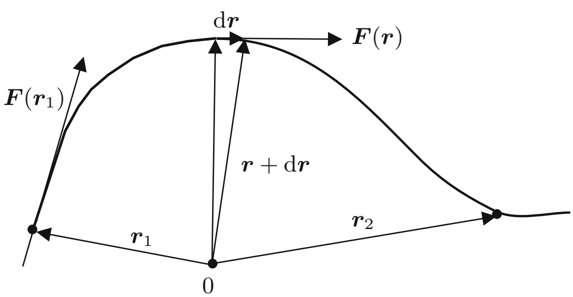

Fig. B.3 Lines of force for the vector field $\boldsymbol{F}(\boldsymbol{r})$

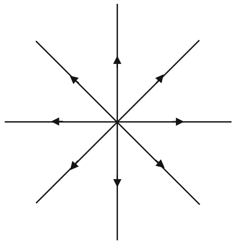

Fig. B.4 Lines of force of the vector field $\boldsymbol{F}(\boldsymbol{r}) = \boldsymbol{r}/r^3$

and

$$\boldsymbol{r} \times \mathrm{d}\boldsymbol{r} = \begin{vmatrix} \boldsymbol{e}_x & \boldsymbol{e}_y & \boldsymbol{e}_z \\ x & y & z \\ \mathrm{d}x & \mathrm{d}y & \mathrm{d}z \end{vmatrix} = \begin{pmatrix} y\,\mathrm{d}z - z\,\mathrm{d}y \\ z\,\mathrm{d}x - x\,\mathrm{d}z \\ x\,\mathrm{d}y - y\,\mathrm{d}x \end{pmatrix} . \tag{B.6}$$

Therefore, we can formulate the following three relations

$$y\,\mathrm{d}z = z\,\mathrm{d}y \tag{B.7}$$

$$z\,\mathrm{d}x = x\,\mathrm{d}z \tag{B.8}$$

$$x\,\mathrm{d}y = y\,\mathrm{d}x . \tag{B.9}$$

We now search for the line of force including point $P_0(x_0, y_0, z_0)$. Integration of (B.7) results in

$$\ln \frac{y}{y_0} = \ln \frac{z}{z_0} \tag{B.10}$$

and

$$z_0 y = y_0 z . \tag{B.11}$$

Analogously, we can compute the solutions of the other two differential equations

$$z_0 x = x_0 z \tag{B.12}$$

$$y_0 x = x_0 y . \tag{B.13}$$

From (B.12) a plane through point P_0 containing the y-axis, and from (B.13) a plane through point P_0 containing the z-axis is defined. The intersection of the two planes leads to a straight line through the origin, and therefore we obtain the vector field drawn in Fig. B.4, which corresponds, e.g., to the vector field of an electric charge.

B.1 The Nabla (∇) Operator

First, we recall that a scalar function may depend on one or more variables, e.g., using Cartesian coordinates, a function can be denoted by

$$f = f(x, y, z) .$$

The partial derivatives read as

$$\frac{\partial f}{\partial x}, \quad \frac{\partial f}{\partial y}, \quad \frac{\partial f}{\partial z}\,.$$

The nabla operator ∇ is defined in Cartesian coordinates by

$$\nabla = \frac{\partial}{\partial x}\boldsymbol{e}_x + \frac{\partial}{\partial y}\boldsymbol{e}_y + \frac{\partial}{\partial z}\boldsymbol{e}_z = \begin{pmatrix} \frac{\partial}{\partial x} \\ \frac{\partial}{\partial y} \\ \frac{\partial}{\partial z} \end{pmatrix}, \tag{B.14}$$

where $\boldsymbol{e}_x$, $\boldsymbol{e}_y$ and $\boldsymbol{e}_z$ are the unit vectors in x-, y-, and z-directions. The interaction between the nabla operator and a scalar or a vector field yields its geometric significance.

B.2 Definition of Gradient, Divergence, and Curl

We introduce a scalar function V with nonzero first-order partial derivatives with respect to the coordinates x, y, and z, and a vector field $\boldsymbol{F}$ with components F_x, F_y, and F_z. Then, the following operations are defined:

1. *Gradient of a scalar:*

$$\textbf{grad}\ V = \nabla V = \begin{pmatrix} \frac{\partial V}{\partial x} \\ \frac{\partial V}{\partial y} \\ \frac{\partial V}{\partial z} \end{pmatrix}.$$

   As can be seen, the result of this operation is a vector.

2. *Divergence of a vector:*

$$\textbf{div}\,\boldsymbol{F} = \nabla \cdot \boldsymbol{F} = \frac{\partial F_x}{\partial x} + \frac{\partial F_y}{\partial y} + \frac{\partial F_z}{\partial z}\,.$$

   Therefore, the result of this operation is a scalar value.

3. *Curl of a vector:*

$$\textbf{curl}\ \boldsymbol{F} = \nabla \times \boldsymbol{F} = \begin{vmatrix} \boldsymbol{e}_x & \boldsymbol{e}_y & \boldsymbol{e}_z \\ \partial/\partial x & \partial/\partial y & \partial/\partial z \\ F_x & F_y & F_z \end{vmatrix} = \begin{pmatrix} \frac{\partial F_z}{\partial y} - \frac{\partial F_y}{\partial z} \\ \frac{\partial F_x}{\partial z} - \frac{\partial F_z}{\partial x} \\ \frac{\partial F_y}{\partial x} - \frac{\partial F_x}{\partial y} \end{pmatrix}.$$

   The result of taking the **curl** of a vector is again a vector.

B.3 The Gradient

We will consider the scalar function $V(x, y, z)$ with its partial derivatives $\partial V/\partial x$, $\partial V/\partial y$, $\partial V/\partial z$ and dependent on a point $\mathbf{P} = (x, y, z)$. In the first step we calculate the total differential of V

$$\mathrm{d}V = \frac{\partial V}{\partial x}\mathrm{d}x + \frac{\partial V}{\partial y}\mathrm{d}y + \frac{\partial V}{\partial z}\mathrm{d}z\,. \tag{B.15}$$

Now, we define a point $\boldsymbol{P}'$ infinitely close to $\boldsymbol{P}$ by $\boldsymbol{P}' = (x+\mathrm{d}x, y+\mathrm{d}y, z+dz)$. By calculating the vector $d\boldsymbol{P} = \boldsymbol{P}' - \boldsymbol{P}$, which has the components $d\boldsymbol{P} = (\mathrm{d}x, \mathrm{d}y, dz)^T$, we can write (B.15) as

$$\begin{aligned}\mathrm{d}V &= \left(\frac{\partial V}{\partial x}\boldsymbol{e}_x + \frac{\partial V}{\partial y}\boldsymbol{e}_y + \frac{\partial V}{\partial z}\boldsymbol{e}_z\right)\cdot\left(\mathrm{d}x\boldsymbol{e}_x + \mathrm{d}y\boldsymbol{e}_y + \mathrm{d}z\boldsymbol{e}_z\right) &\text{(B.16)}\\ &= \nabla V \cdot \mathrm{d}\boldsymbol{P}\,. &\text{(B.17)}\end{aligned}$$

For the geometrical illustration of the gradient, consider an equipotential surface, i.e., a surface with $V = const.$ (see Fig. B.5). Hence, for all differential displacements from $\boldsymbol{P}$ to $\boldsymbol{P}'$ on this surface $dV = 0$ holds, and therefore,

$$\nabla V \cdot \mathrm{d}\boldsymbol{P} = 0\,. \tag{B.18}$$

From the definition of the scalar product it is clear that ∇V and $d\boldsymbol{P}$ are orthogonal. In this situation the displacement from $\boldsymbol{P}$ to $\boldsymbol{P}'$ points into the direction of increasing V, as shown in Fig. B.6, and the scalar product $\nabla V \cdot \mathrm{d}\boldsymbol{P}$ is positive.

From the foregoing arguments, we conclude that ∇V is a vector, perpendicular to the surface on which V is constant and that it points in the direction of increasing V.

As an example we consider a function $r(x, y, z)$, which defines the distance of a point $\boldsymbol{P}$ from the origin (0, 0, 0). The surface $r = const.$ is a sphere of radius r with center (0, 0, 0), whose equation is given by

$$r = \sqrt{x^2 + y^2 + z^2}\,.$$

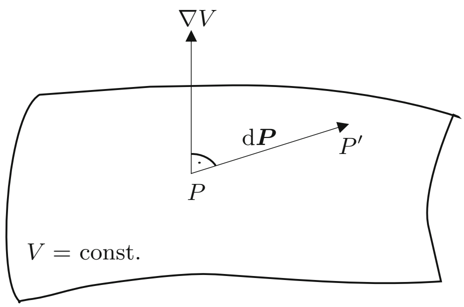

Fig. B.5 The gradient is orthogonal to a constant potential surface

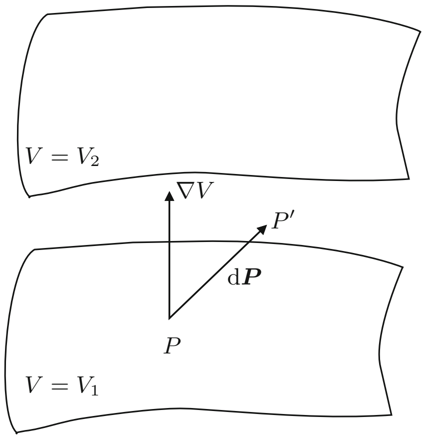

Fig. B.6 Geometrical representation of the gradient

Therefore, the gradient calculates as

$$\frac{\partial r}{\partial x} = \frac{x}{\sqrt{x^2 + y^2 + z^2}} = \frac{x}{r}$$
$$\frac{\partial r}{\partial y} = \frac{y}{r}$$
$$\frac{\partial r}{\partial z} = \frac{z}{r}$$
$$\nabla r = \frac{x\boldsymbol{e}_x + y\boldsymbol{e}_y + z\boldsymbol{e}_z}{r} = \frac{\boldsymbol{r}}{r} .$$

Geometrically speaking, ∇r points in the direction of increasing r, or towards spheres with radii larger than r.

B.4 The Flux

Definition B.3 (*Flux*) The vector field $\boldsymbol{F}(\boldsymbol{r})$ and a corresponding surface Γ as shown in Fig. B.7 are given. The vector $\boldsymbol{n}$ denotes the normal unit vector of the differential surface $d\boldsymbol{\Gamma}$. Therefore, the differential flux $d\psi$ through $d\boldsymbol{\Gamma}$ is defined by

$$\mathrm{d}\psi = \boldsymbol{F} \cdot \mathrm{d}\boldsymbol{\Gamma} = \boldsymbol{F} \cdot \boldsymbol{n}\mathrm{d}\Gamma . \tag{B.19}$$

The total flux ψ computes as

$$\psi = \int_{\Gamma} \boldsymbol{F} \cdot \mathrm{d}\boldsymbol{\Gamma} . \tag{B.20}$$

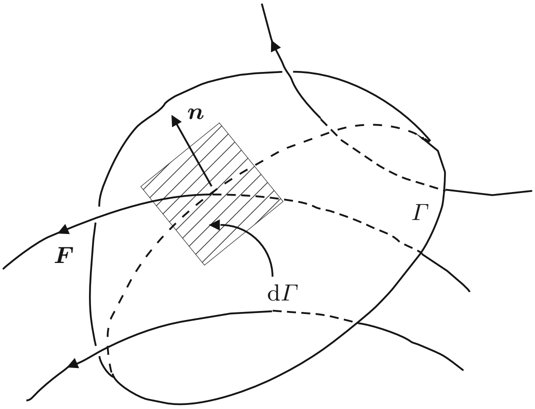

Fig. B.7 Flux through the surface Γ

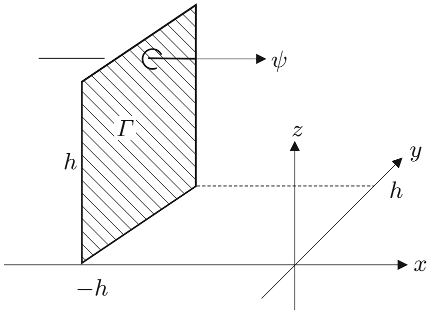

Fig. B.8 Flux ψ through the square with area h^2

In the following, we want to compute the flux ψ of the vector field $\boldsymbol{F}(\boldsymbol{r}) = \boldsymbol{r}$ through the square Γ with side length h according to Fig. B.8. With the normal unit vector $\boldsymbol{n} = \boldsymbol{e}_x$ and $d\boldsymbol{\Gamma} = \mathrm{d}y\,\mathrm{d}z\boldsymbol{e}_x$ we obtain

$$\begin{aligned}\psi &= \int_0^h \int_0^h \left(-h\boldsymbol{e}_x + y\boldsymbol{e}_y + z\boldsymbol{e}_z\right) \cdot \boldsymbol{e}_x \,\mathrm{d}y\,\mathrm{d}z \\ &= -h \int_0^h \int_0^h \mathrm{d}y dz \\ &= -h^3 . \end{aligned} \tag{B.21}$$

The total flux ψ through a closed surface S is given by

$$\psi = \oint_\Gamma \boldsymbol{F} \cdot \mathrm{d}\boldsymbol{\Gamma} \tag{B.22}$$

and defines whether we have sources ($\psi > 0$) or sinks ($\psi < 0$) within Γ.

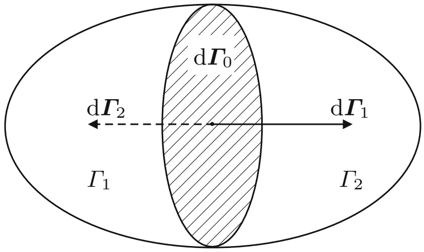

Fig. B.9 Flux through the closed surface $\Gamma_1 \cup \Gamma_2$

A very important property of the flux ψ defined by a closed surface is given by (see Fig. B.9)

$$\oint\limits_{\Gamma_1 \cup \Gamma_0} \boldsymbol{F} \cdot \mathrm{d}\boldsymbol{\Gamma} + \oint\limits_{\Gamma_2 \cup \Gamma_0} \boldsymbol{F} \cdot \mathrm{d}\boldsymbol{\Gamma} = \oint\limits_{\Gamma_1 \cup \Gamma_2} \boldsymbol{F} \cdot \mathrm{d}\boldsymbol{\Gamma} \,. \tag{B.23}$$

B.5 Divergence

Definition B.4 (*Divergence*) The vector field $\boldsymbol{F}(\boldsymbol{r})$ is given. If we divide the flux ψ, defined by a closed surface Γ, by the corresponding volume Ω and let the volume Ω tend to zero, then the obtained value is called the divergence (source density)

$$\mathbf{div}\, \boldsymbol{F} = \lim_{\Omega \to 0} \frac{1}{\Omega} \oint_{\Gamma} \boldsymbol{F} \cdot \mathrm{d}\boldsymbol{\Gamma} = \left. \frac{\mathrm{d}\psi}{\mathrm{d}\Omega} \right|_{\boldsymbol{r}} . \tag{B.24}$$

Let us now consider the closed surface of a differential cube (see Fig. B.10) and the general vector field $\boldsymbol{F}(\boldsymbol{r}) = F_x \boldsymbol{e}_x + F_y \boldsymbol{e}_y + F_z \boldsymbol{e}_z$. In the first step, let us compute the differential flux through the hatched surfaces

$$\begin{aligned} \boldsymbol{F} \cdot \mathrm{d}\boldsymbol{\Gamma} &= [\boldsymbol{F}(x + \mathrm{d}x/2, y, z) - \boldsymbol{F}(x - \mathrm{d}x/2, y, z)] \cdot \boldsymbol{e}_x \mathrm{d}y\, \mathrm{d}z \\ &\approx \left[F_x(x, y, z) + \frac{\partial F_x}{\partial x} \frac{\mathrm{d}x}{2} - \left(F_x(x, y, z) - \frac{\partial F_x}{\partial x} \frac{\mathrm{d}x}{2} \right) \right] \mathrm{d}y\, \mathrm{d}z \\ &= \frac{\partial F_x}{\partial x} \mathrm{d}x\, \mathrm{d}y\, \mathrm{d}z \,. \end{aligned} \tag{B.25}$$

Analogously, we obtain the contribution of the other two directions, and thus, the differential flux

$$\mathrm{d}\psi = \left(\frac{\partial F_x}{\partial x} + \frac{\partial F_y}{\partial y} + \frac{\partial F_z}{\partial z} \right) \mathrm{d}x\, \mathrm{d}y\, \mathrm{d}z \,. \tag{B.26}$$

Since the differential volume $\mathrm{d}\Omega$ is equal to $\mathrm{d}x\, \mathrm{d}y\, \mathrm{d}z$, we end up with the following expression for the divergence of a vector field in Cartesian coordinates

$$\mathbf{div}\, \boldsymbol{F} = \frac{\partial F_x}{\partial x} + \frac{\partial F_y}{\partial y} + \frac{\partial F_z}{\partial z} \,, \tag{B.27}$$

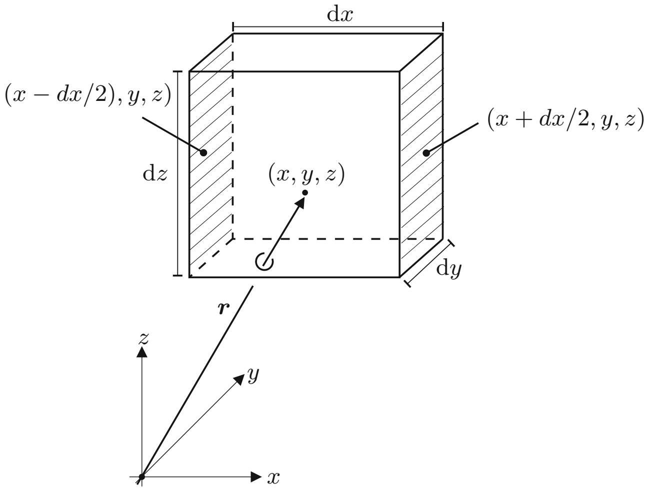

Fig. B.10 Flux through a cube

or, by using the nabla operator,

$$\mathbf{div}\, \boldsymbol{F} = \nabla \cdot \boldsymbol{F}\,. \tag{B.28}$$

B.6 Divergence Theorem (Gauss Theorem)

By the definition of the divergence (see B.24) we get

$$\mathrm{d}\psi = \nabla \cdot \boldsymbol{F}\, \mathrm{d}\Omega \tag{B.29}$$

$$\psi = \int_{\Omega} \nabla \cdot \boldsymbol{F}\, \mathrm{d}\Omega\,. \tag{B.30}$$

On the other hand, we have the relation for the flux ψ according to (B.22). Combining these two expressions for the flux results in

$$\psi = \int_{\Omega} \nabla \cdot \boldsymbol{F}\, \mathrm{d}\Omega = \oint_{\Gamma(\Omega)} \boldsymbol{F} \cdot \mathrm{d}\boldsymbol{\Gamma}\,. \tag{B.31}$$

This equality between the two integrals tells us that the flux of the vector $\boldsymbol{F}$ through the closed surface Γ is equal to the volume integral of the divergence of $\boldsymbol{F}$ over the volume Ω enclosed by the surface Γ.

Consider a radial vector field $\boldsymbol{F}$ as shown in Fig. B.11, and assume that the magnitude of $\boldsymbol{F}$ is constant in all points on a sphere centered at P. To compute the flux of the vector field $\boldsymbol{F}$ through a spherical shell of radius R, we note that $d\boldsymbol{s}$ and

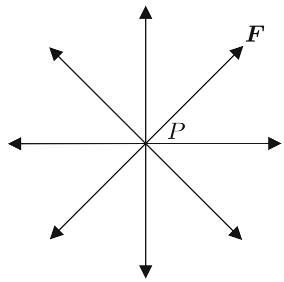

Fig. B.11 Radial vector field

$\boldsymbol{F}$ are collinear and in the same direction

$$\psi = \oint_S \boldsymbol{F} \cdot \mathrm{d}\boldsymbol{\Gamma} = F \oint_\Gamma \mathrm{d}\Gamma = 4\pi R^2 F\,.$$

From the divergence theorem, (the flux is nonzero) we conclude

$$\nabla \cdot \boldsymbol{F} \neq 0\,.$$

B.7 The Circulation

The circulation of a vector field $\boldsymbol{F}(\boldsymbol{r})$ along a closed contour C is given by the closed-line integral

$$Z = \oint_C \boldsymbol{F} \cdot \mathrm{d}\boldsymbol{s}\,. \tag{B.32}$$

Therefore, the important property follows (see Fig. B.12)

$$\oint_{C_1 \cup C_0} \boldsymbol{F} \cdot \mathrm{d}\boldsymbol{r} + \oint_{C_2 \cup C_0} \boldsymbol{F} \cdot \mathrm{d}\boldsymbol{r} = \oint_{C_1 \cup C_2} \boldsymbol{F} \cdot \mathrm{d}\boldsymbol{r}\,. \tag{B.33}$$

If the circulation along a closed curve C is not equal to zero, then we say the closed line contains eddies.

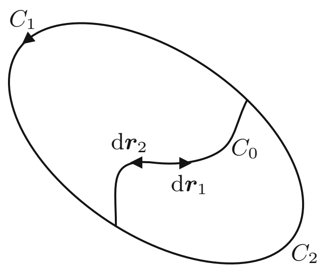

Fig. B.12 Circulation along the closed line $C_1 \cup C_2$

B.8 The Curl

Definition B.5 (*Curl*) We consider a point defined by $\boldsymbol{r}$ (Fig. B.13), in which the curl of the vector field $\boldsymbol{F}$ has to be computed. Furthermore, we define a closed line C enclosing the area Γ and consider the circulation along C. If the area Γ tends to zero, we obtain the definition of the curl by

$$\boldsymbol{n} \cdot \textbf{curl}\ \boldsymbol{F} = \lim_{\Gamma \to 0} \frac{\oint_C \boldsymbol{F} \cdot \mathrm{d}\boldsymbol{s}}{\Gamma} = \frac{\mathrm{d}Z}{\mathrm{d}\Gamma}\,. \tag{B.34}$$

The vector curl $\boldsymbol{F}$ is obtained by a separation in the three directions of the unit vectors $\boldsymbol{e}_x$, $\boldsymbol{e}_y$, and $\boldsymbol{e}_z$

$$\textbf{curl}\ \boldsymbol{F} = (\boldsymbol{e}_x \cdot \textbf{curl}\ \boldsymbol{F})\boldsymbol{e}_x + (\boldsymbol{e}_y \cdot \textbf{curl}\ \boldsymbol{F})\boldsymbol{e}_y + (\boldsymbol{e}_z \cdot \textbf{curl}\ \boldsymbol{F})\boldsymbol{e}_z\,. \tag{B.35}$$

The circulation for the differential square in Fig. B.14 is given by

$$\begin{aligned} \mathrm{d}Z_x &= (\boldsymbol{F}(x, y, z - \mathrm{d}z/2) - \boldsymbol{F}(x, y, z + \mathrm{d}z/2)) \cdot \boldsymbol{e}_y\ \mathrm{d}y \\ &+\ (\boldsymbol{F}(x, y + \mathrm{d}y/2, z) - \boldsymbol{F}(x, y - \mathrm{d}y/2, z)) \cdot \boldsymbol{e}_z\ \mathrm{d}z \\ &\approx \left(\frac{\partial F_z}{\partial y} - \frac{\partial F_y}{\partial z}\right) \mathrm{d}y dz\,. \end{aligned} \tag{B.36}$$

Therefore, we obtain the x-component of curl $\boldsymbol{F}$ with $\mathrm{d}\Gamma = \mathrm{d}y\,\mathrm{d}z$

$$\boldsymbol{e}_x \cdot \textbf{curl}\ \boldsymbol{F} = \frac{\partial F_z}{\partial y} - \frac{\partial F_y}{\partial z}\,. \tag{B.37}$$

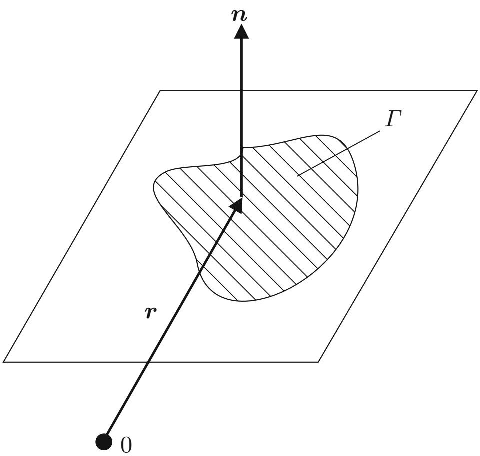

Fig. B.13 Curl in a point defined by $\boldsymbol{r}$

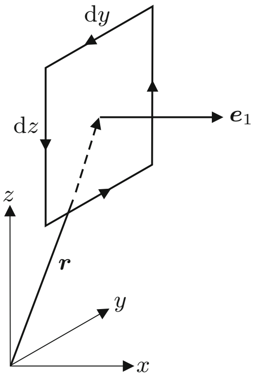

Fig. B.14 x-component of curl $\boldsymbol{F}$

Analogously, the y- and z-component of curl $\boldsymbol{F}$ can be computed, and the full vector in Cartesian coordinates reads as

$$\textbf{curl } \boldsymbol{F} = \begin{pmatrix} \frac{\partial F_z}{\partial y} - \frac{\partial F_y}{\partial z} \\ \frac{\partial F_x}{\partial z} - \frac{\partial F_z}{\partial x} \\ \frac{\partial F_y}{\partial x} - \frac{\partial F_x}{\partial y} \end{pmatrix}, \tag{B.38}$$

or with the help of the nabla operator

$$\textbf{curl } \boldsymbol{F} = \nabla \times \boldsymbol{F} = \begin{vmatrix} \boldsymbol{e}_x & \boldsymbol{e}_y & \boldsymbol{e}_z \\ \frac{\partial}{\partial x} & \frac{\partial}{\partial y} & \frac{\partial}{\partial z} \\ F_x & F_y & F_z \end{vmatrix}. \tag{B.39}$$

B.9 Stoke's Theorem

We consider the vector field $\boldsymbol{F}$ on the surface Γ with fixed oriented contour C as shown in Fig. B.15. For a differential surface $d\Gamma_\nu$, we obtain according to (B.34)

$$\begin{aligned} \mathrm{d}Z_\nu &= \boldsymbol{n}(\boldsymbol{r}_\nu) \cdot \textbf{curl } \boldsymbol{F}(\boldsymbol{r}) \mathrm{d}\Gamma_\nu \\ Z_\nu &= \int\limits_{\Gamma_\nu} \textbf{curl } \boldsymbol{F}(\boldsymbol{r}) \cdot \mathrm{d}\boldsymbol{\Gamma}_\nu \,, \end{aligned} \tag{B.40}$$

and

$$Z = \int_\Gamma \textbf{curl } \boldsymbol{F} \cdot \mathrm{d}\boldsymbol{\Gamma} \,. \tag{B.41}$$

Furthermore, according to the definition of the circulation Z (see B.32), we get the following relation

$$Z = \oint_C \boldsymbol{F} \cdot \mathrm{d}\boldsymbol{r} = \int_\Gamma \textbf{curl } \boldsymbol{F} \cdot \mathrm{d}\boldsymbol{\Gamma} \,. \tag{B.42}$$

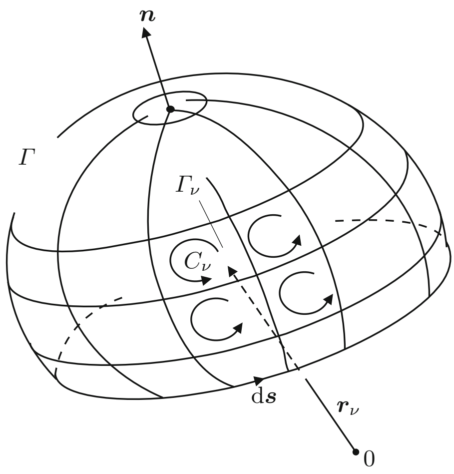

Fig. B.15 Vector field $\boldsymbol{F}$ on the surface Γ with fixed oriented contour C

For a radial vector field $\boldsymbol{F}$ as shown in Fig. B.11, the closed-line integral along a circle C of constant radius

$$\oint_C \boldsymbol{F} \cdot \mathrm{d}\boldsymbol{s}$$

is zero, and therefore, the curl of this vector field $\nabla \times \boldsymbol{F}$ is zero, too.

B.10 Green's Integral Theorems

The integral theorems of Green can be derived from the divergence theorem. For this purpose, we first introduce the Laplace operator by

$$\Delta = \nabla \cdot \nabla = \frac{\partial^2}{\partial x^2} + \frac{\partial^2}{\partial y^2} + \frac{\partial^2}{\partial z^2}\,. \tag{B.43}$$

This differential operator can be applied to scalar as well as vector quantities

$$\Delta V = \mathbf{div}\ (\mathbf{grad}\ V) \tag{B.44}$$

$$\Delta \boldsymbol{F} = (\Delta F_x)\boldsymbol{e}_x + (\Delta F_y)\boldsymbol{e}_y + (\Delta F_z)\boldsymbol{e}_z\,. \tag{B.45}$$

Setting a vector $\boldsymbol{F}$ equal to $V_1 \nabla V_2$ and using the divergence theorem, we obtain according to (B.31)

$$\int_\Omega \nabla \cdot (V_1 \nabla V_2) \mathrm{d}\Omega = \oint_\Gamma (V_1 \nabla V_2) \cdot \mathrm{d}\boldsymbol{\Gamma}\,. \tag{B.46}$$

Since the term $\nabla \cdot (V_1 \nabla V_2)$ can be expressed by (see B.53 below)

$$\nabla \cdot (V_1 \nabla V_2) = V_1 \Delta V_2 + \nabla V_1 \cdot \nabla V_2 \,, \tag{B.47}$$

we get the following integral theorem, called Green's first integral theorem

$$\int_\Omega V_1 \Delta V_2 \mathrm{d}\Omega + \int_\Omega \nabla V_1 \cdot \nabla V_2 \mathrm{d}\Omega = \oint_\Gamma V_1 \frac{\partial V_2}{\partial n} \mathrm{d}\Gamma \,. \tag{B.48}$$

By substituting V_1 with V_2 and vice versa in (B.46) and subtracting the resulting equation from (B.46), we achieve Green's second integral theorem

$$\int_\Omega V_1 \Delta V_2 \mathrm{d}\Omega - \int_\Omega V_2 \Delta V_1 \mathrm{d}\Omega = \oint_\Gamma \left(V_1 \frac{\partial V_2}{\partial n} - V_2 \frac{\partial V_1}{\partial n} \right) \mathrm{d}\Gamma \,. \tag{B.49}$$

In addition, Green's first integral theorem in vector form is

$$\int_\Omega \left(\nabla \times \boldsymbol{u} \cdot \nabla \times \boldsymbol{v} - \boldsymbol{u} \cdot \nabla \times \nabla \times \boldsymbol{v} \right) \mathrm{d}\Omega = \int_\Gamma (\boldsymbol{u} \times \nabla \times \boldsymbol{v}) \cdot \boldsymbol{n} \mathrm{d}\Gamma \,, \tag{B.50}$$

and Green's second integral theorem in vector form reads as

$$\int_\Omega \left(\boldsymbol{u} \cdot \nabla \times \nabla \times \boldsymbol{v} - \boldsymbol{v} \cdot \nabla \times \nabla \times \boldsymbol{u} \right) \mathrm{d}\Omega = \int_\Gamma (\boldsymbol{v} \times \nabla \times \boldsymbol{u} - \boldsymbol{u} \times \nabla \times \boldsymbol{v}) \cdot \boldsymbol{n} \mathrm{d}\Gamma \,. \tag{B.51}$$

B.11 Application of the Operators

By using the definitions of gradient, divergence, and curl in Cartesian coordinates, the following relations hold:

$$\nabla(V_1 V_2) = V_1 \nabla V_2 + V_2 \nabla V_1 \tag{B.52}$$

$$\nabla \cdot (V\boldsymbol{F}) = V \nabla \cdot \boldsymbol{F} + \boldsymbol{F} \cdot \nabla V \tag{B.53}$$

$$\nabla \cdot (\boldsymbol{F}_1 \times \boldsymbol{F}_2) = \boldsymbol{F}_2 \cdot \nabla \times \boldsymbol{F}_1 - \boldsymbol{F}_1 \cdot \nabla \times \boldsymbol{F}_2 \tag{B.54}$$

$$\nabla \times (V\boldsymbol{F}) = V \nabla \times \boldsymbol{F} - \boldsymbol{F} \times \nabla V \tag{B.55}$$

$$\Delta \boldsymbol{F} = \nabla(\nabla \cdot \boldsymbol{F}) - \nabla \times (\nabla \times \boldsymbol{F}) \,. \tag{B.56}$$

These relations combine the essential differential operators and build up a basis for the description of physical fields.

B.12 Irrotational Vector Fields

We consider a vector field $\boldsymbol{F}$, which is given as the gradient of a scalar potential $\boldsymbol{F} = \nabla V$. The computation of a line integral from point A to point B yields

$$\int_A^B (\nabla V) \cdot \mathrm{d}\boldsymbol{r} = V(B) - V(A)\,. \tag{B.57}$$

Therefore, for any closed contour within this vector field, the following relation holds

$$\oint (\nabla V) \cdot \mathrm{d}\boldsymbol{r} = 0\,. \tag{B.58}$$

This result proves that any vector field that can be expressed by the gradient of a scalar potential is irrotational. Furthermore, the local quantity, given by the curl of the vector field, is zero

$$\nabla \times \nabla V = 0\,. \tag{B.59}$$

B.13 Solenoidal Vector Fields

We will consider the solenoidal vector field $\nabla \times \boldsymbol{F}$ for a domain as displayed in Fig. B.16. This domain shall consist of two subdomains defined by their surfaces Γ_1 and Γ_2 with their related contours C_1 and C_2. By using Stoke's theorem, we obtain the following relation

$$\begin{aligned}\oint_{\Gamma} (\nabla \times \boldsymbol{F}) \cdot \mathrm{d}\boldsymbol{\Gamma} &= \oint_{\Gamma_1} (\nabla \times \boldsymbol{F}) \cdot \boldsymbol{n}_1\,\mathrm{d}\Gamma + \oint_{\Gamma_2} (\nabla \times \boldsymbol{F}) \cdot \boldsymbol{n}_2\,\mathrm{d}\Gamma \\ &= \oint_{C_1} \boldsymbol{F} \cdot \mathrm{d}\boldsymbol{r} + \oint_{C_2} \boldsymbol{F} \cdot \mathrm{d}\boldsymbol{r} \\ &= 0\,. \end{aligned} \tag{B.60}$$

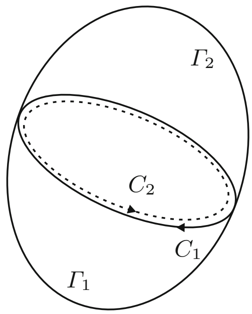

Fig. B.16 Domain for solenoidal vector field

Thus, the total flux (global quantity) is zero, and, furthermore, the local solenoidality, too

$$\nabla \cdot (\nabla \times \boldsymbol{F}) = 0\,. \tag{B.61}$$

Appendix C
Tensors and Index Notation

Tensors are simply speaking a linear mapping. E.g., a second order tensor $[\boldsymbol{A}]$ is a linear mapping that associates a given vector $\boldsymbol{u}$ with a second vector $\boldsymbol{v}$ by

$$\boldsymbol{v} = [\boldsymbol{S}]\boldsymbol{u} \,.$$

The term linear in the above relation implies that given two arbitrary vectors $\boldsymbol{u}$ and $\boldsymbol{v}$ and two arbitrary scalars α, β, then the following relation holds

$$[\boldsymbol{S}]\,(\alpha\boldsymbol{u} + \beta\boldsymbol{v}) = \alpha[\boldsymbol{S}]\boldsymbol{u} + \beta[\boldsymbol{S}]\boldsymbol{v} \,.$$

The extension to tensors of higher rank is straight forward. E.g., Hook's law maps the mechanical strain tensor $[\boldsymbol{S}]$ by the 4th order elasticity tensor $[\boldsymbol{c}]$ to the mechanical stress tensor $[\boldsymbol{\sigma}]$

$$[\boldsymbol{\sigma}] = [\boldsymbol{c}]\,[\boldsymbol{S}] \,.$$

Now, index notation is a powerful tool to write complex operations of vectors and tensors in a more readable way. However, there are times when the more conventional vector notation is more useful. It is therefore important to be able to easily convert back and forth between the two notations. Table C.1 describes our notation.[1] An index can be a *free* or a *dummy* index. For free indices, the following rules are defined:

- The number of free indices equals the rank as displayed in Table C.1. Thereby, a scalar is a tensor with rank 0, and a vector is a tensor of rank 1. Tensors may assume a rank of any integer greater than or equal to zero. Please note that it is just allowed to sum together tensors with equal rank.
- A free index appears once and only once within each additive term and remains within the expression after the operation has been performed, e.g.

$$a_i = \epsilon_{ijk} b_j c_k + A_{ij} d_j \,. \tag{C.1}$$

[1] Our notation does not differ between tensors of different orders.

M. Kaltenbacher, *Numerical Simulation of Mechatronic Sensors and Actuators*,
DOI 10.1007/978-3-642-40170-1

Table C.1 Vector and index notation

	Vector	Index	Rank
Scalar	ξ	ξ	0
Vector	$\boldsymbol{u}$	u_i	1
Tensor (2nd order)	$[\boldsymbol{A}]$	A_{ij}	2
Tensor (3rd order)	$[\boldsymbol{B}]$	B_{ijk}	3
Tensor (4th order)	$[\boldsymbol{C}]$	C_{ijkl}	4

- The same letter must be used for the free index in every additive term.
- The first free index in a term corresponds to the row, and the second corresponds to the column. Thus, a vector (which has only one free index) is written as a column of three rows

$$\boldsymbol{u} = u_i = \begin{pmatrix} u_1 \\ u_2 \\ u_3 \end{pmatrix}$$

and a second order tensor as

$$[\boldsymbol{A}] = A_{ij} = \begin{pmatrix} A_{11} & A_{12} & A_{13} \\ A_{21} & A_{22} & A_{23} \\ A_{31} & A_{32} & A_{33} \end{pmatrix}$$

A dummy index defines an index, which does not appear in the final expression any more. The rules are as follows:

- A dummy index appears twice within an additive term of an expression. For the example above (see (C.1)), the dummy indices are j and k.
- A dummy index implies a summation over the range of the index, e.g.

$$a_{ii} = a_{11} + a_{22} + a_{33} \,.$$

For many operations we use the Kronecker delta (2nd order tensor)

$$\delta_{ij} = \begin{pmatrix} 1 & 0 & 0 \\ 0 & 1 & 0 \\ 0 & 0 & 1 \end{pmatrix} \tag{C.2}$$

and the alternating unit tensor (3rd order tensor)

$$\epsilon_{ijk} = \begin{cases} 1 & \text{if } ijk = 123,\ 231 \text{ or } 312 \\ 0 & \text{if any two indices are the same} \\ -1 & \text{if } ijk = 132,\ 213 \text{ or } 3321 \end{cases} \tag{C.3}$$

Thereby, the following relation can be explored

$$\epsilon_{ijk} = \frac{1}{2}(i-j)\,(j-k)\,(k-i)\,.$$

With these definitions, we may write vector and tensor operations using index notation. Here, we list the most useful ones:

- Scalar product of two vectors

$$\boldsymbol{a} \cdot \boldsymbol{b} = c \;\rightarrow\; a_i b_i = c \tag{C.4}$$

- Vector product of two vectors

$$\boldsymbol{a} \times \boldsymbol{b} = \boldsymbol{c} \;\rightarrow\; \epsilon_{ijk} a_j b_k = c_i \tag{C.5}$$

- Gradient of a scalar

$$\nabla \phi = \boldsymbol{u} \;\rightarrow\; \frac{\partial \phi}{\partial x_i} = u_i \tag{C.6}$$

- Gradient of a vector

$$\nabla \boldsymbol{a} = \begin{pmatrix} \frac{\partial a_1}{\partial x_1} & \frac{\partial a_2}{\partial x_1} & \frac{\partial a_3}{\partial x_1} \\ \frac{\partial a_1}{\partial x_2} & \frac{\partial a_2}{\partial x_2} & \frac{\partial a_3}{\partial x_2} \\ \frac{\partial a_1}{\partial x_3} & \frac{\partial a_2}{\partial x_3} & \frac{\partial a_3}{\partial x_3} \end{pmatrix} \rightarrow \frac{\partial a_i}{\partial x_j} \tag{C.7}$$

- Gradient of a second order tensor

$$\nabla [\boldsymbol{A}] = \frac{\partial [\boldsymbol{A}]}{\partial \boldsymbol{x}} = \sum_{i,j,k=1}^{3} \frac{\partial A_{ij}}{\partial x_k} \boldsymbol{e}_i \otimes \boldsymbol{e}_j \otimes \boldsymbol{e}_k \tag{C.8}$$

- Divergence of a vector

$$\nabla \cdot \boldsymbol{a} = b \;\rightarrow\; \frac{\partial a_i}{\partial x_i} = b \tag{C.9}$$

- Divergence of a second order tensor

$$\nabla \cdot [\boldsymbol{A}] = \sum_{i,j=1}^{3} \frac{\partial A_{ij}}{\partial x_j} \boldsymbol{e}_i \tag{C.10}$$

- Curl of a vector

$$\nabla \times \boldsymbol{a} = \boldsymbol{b} \;\rightarrow\; \epsilon_{ijk} \frac{\partial a_k}{\partial x_j} = b_i \tag{C.11}$$

- Double product or double contraction of two second order tensors

$$[\boldsymbol{A}] : [\boldsymbol{B}] = c \;\rightarrow\; A_{ij} B_{ij} = c \tag{C.12}$$

  or of a fourth order tensor with a second order tensors, e.g. Hooks law (see Sect. 3.4)

$$[\boldsymbol{\sigma}] = [\boldsymbol{c}] : [\boldsymbol{S}] \tag{C.13}$$

- Dyadic or tensor product

$$\boldsymbol{a} \otimes \boldsymbol{b} = [\boldsymbol{C}] \ \rightarrow \ a_i b_j = C_{ij} \tag{C.14}$$

$$[\boldsymbol{A}] \otimes \boldsymbol{b} = [\boldsymbol{C}] \ \rightarrow \ A_{ij} b_k = C_{ijk} \tag{C.15}$$

$$[\boldsymbol{A}] \otimes [\boldsymbol{B}] = [\boldsymbol{D}] \ \rightarrow \ A_{ij} B_{kl} = D_{ijkl} \tag{C.16}$$

- Product of two tensors

$$[\boldsymbol{A}][\boldsymbol{B}] = [\boldsymbol{C}] \ \rightarrow \ A_{ij} B_{jk} = C_{ik} \tag{C.17}$$

  Note that only the inner index is to be summed.
- Vector product of a second order tensor and a vector

$$\boldsymbol{a}[\boldsymbol{B}] = \boldsymbol{c} \ \rightarrow \ a_i B_{ij} = c_j \tag{C.18}$$

  A typical example is obtaining out of the mechanical stress tensor $[\boldsymbol{\sigma}]$ the stress vector in normal direction, e.g. $\boldsymbol{n}[\boldsymbol{\sigma}] = \boldsymbol{\sigma}_{\mathrm{n}}$. Please note that $\boldsymbol{n}[\boldsymbol{\sigma}] = [\boldsymbol{\sigma}]^T \boldsymbol{n} \neq [\boldsymbol{\sigma}]\boldsymbol{n}$

- Trace of a tensor

$$\mathrm{tr}\left([\boldsymbol{A}]\right) = b \ \rightarrow \ A_{ii} = b \tag{C.19}$$

The transpose of a tensor $[\boldsymbol{A}]$ is defined as the tensor $[\boldsymbol{A}]^T$, which for any two vectors $\boldsymbol{a}$ and $\boldsymbol{b}$ satisfies

$$\boldsymbol{a} \cdot [\boldsymbol{A}]\boldsymbol{b} = \boldsymbol{b} \cdot [\boldsymbol{A}]^T \boldsymbol{a} \,. \tag{C.20}$$

The definition of the transposed for a tensor $[\boldsymbol{c}]$ of 4th order reads as

$$[\boldsymbol{A}] : [\boldsymbol{c}][\boldsymbol{B}] = [\boldsymbol{B}] : [\boldsymbol{c}]^T [\boldsymbol{A}] \,. \tag{C.21}$$

Furthermore, the following relations hold

$$([\boldsymbol{A}][\boldsymbol{B}])^T = [\boldsymbol{B}]^T [\boldsymbol{A}]^T \,; \ (\boldsymbol{a} \otimes \boldsymbol{b})^T = \boldsymbol{b} \otimes \boldsymbol{a} \,; \ ([\boldsymbol{A}] \otimes [\boldsymbol{B}])^T = [\boldsymbol{B}] \otimes [\boldsymbol{A}] \,. \tag{C.22}$$

Tensors that satisfy the property

$$[\boldsymbol{A}]^T [\boldsymbol{A}] = [\boldsymbol{I}] \,, \tag{C.23}$$

where $[\boldsymbol{I}]$ is the identity tensor, are said to be orthogonal. In fact, any second order tensor $[\boldsymbol{T}]$ can be decomposed into a symmetric tensor $[\boldsymbol{S}]$ and into a skew tensor $[\boldsymbol{A}]$

$$[\boldsymbol{T}] = [\boldsymbol{S}] + [\boldsymbol{A}] \,, \tag{C.24}$$

which compute as follows

$$[\boldsymbol{S}] = \frac{1}{2}\left([\boldsymbol{T}] + [\boldsymbol{T}]^T\right) \; ; \; [\boldsymbol{A}] = \frac{1}{2}\left([\boldsymbol{T}] - [\boldsymbol{T}]^T\right) . \tag{C.25}$$

Thereby, the following properties for a general tensor $[\boldsymbol{T}]$ and a symmetric tensor $[\boldsymbol{S}]$ are fulfilled

$$[\boldsymbol{S}] : [\boldsymbol{T}] = [\boldsymbol{S}] : \mathrm{sym}\,([\boldsymbol{T}]) \; ; \; \boldsymbol{a} \cdot [\boldsymbol{T}]\boldsymbol{a} = \boldsymbol{a} \cdot \mathrm{sym}\,([\boldsymbol{T}])\,\boldsymbol{a} . \tag{C.26}$$

Appendix D
Appropriate Function Spaces

Let us define the derivative of order α with respect to the multi-index α, with $|\alpha| = \sum_i \alpha_i$ and $\alpha_i \in \mathbb{N}$, as follows

$$D^\alpha v := \frac{\partial^{|\alpha|} v}{\partial x_1^{\alpha_1} \cdots x_n^{\alpha_n}} \,. \tag{D.1}$$

For example, the partial derivatives of order 2 in $\mathbb{R}^2$ can be written as $D^\alpha v$ with $\alpha = (2, 0)$, $\alpha = (1, 1)$ or $\alpha = (0, 2)$, since $|\alpha| = \alpha_1 + \alpha_2 = 2$ is fulfilled for all three cases

$$\begin{aligned} \alpha = (2,0) \qquad & D^\alpha v = \frac{\partial^2 v}{\partial x_1^2} \\ \alpha = (1,1) \qquad & D^\alpha v = \frac{\partial^2 v}{\partial x_1 \partial x_2} \\ \alpha = (0,2) \qquad & D^\alpha v = \frac{\partial^2 v}{\partial x_2^2} \,. \end{aligned}$$

Definition D.1 *Continuously differentiable functions*: Let Ω be a closed domain in $\mathbb{R}^n$ and let $C(\Omega)$ denote the space of continuous functions on Ω. Now, the space of up to order m continuously differentiable functions is given by

$$C^m(\Omega) = \left\{ v : \Omega \to \mathbb{R} \mid D^\alpha v \in C(\Omega), |\alpha| \le m \right\} \,. \tag{D.2}$$

If the function v is infinitely often continuously differentiable on Ω, we write $v \in C^\infty(\Omega)$.

For the function $u(x)$ shown Fig. D.1 the following inclusions hold (with $v(x) = u'(x)$)

$$\begin{aligned} v &\in C^0 \\ u &\in C^1 \,. \end{aligned}$$

M. Kaltenbacher, *Numerical Simulation of Mechatronic Sensors and Actuators*,
DOI 10.1007/978-3-642-40170-1

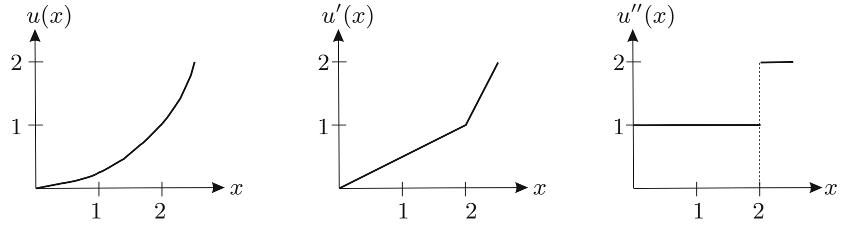

Fig. D.1 Example of a C^1 function

Definition D.2 *Square integrable functions*: Let Ω be a closed domain in $\mathbb{R}^n$. Then, the function u is called square integrable, if it fulfills the following relation

$$\int_{\Omega} |u(x)|^2 \, \mathrm{d}x < \infty \,. \tag{D.3}$$

We denote

$$L_2(\Omega) = \{u : \Omega \to \mathbb{R} \mid \int_{\Omega} \mid u(x) \mid^2 \mathrm{d}x < \infty\} \,. \tag{D.4}$$

For example, the function $f(t)$ with the definition

$$f(t) = \begin{cases} 1 & \text{for} \quad 0 < x < 2 \\ 0 & \text{for} \quad x = 0 \\ -1 & \text{for} \quad -2 \leq x < 0 \end{cases} \tag{D.5}$$

belongs to the space $L_2(-2, 2)$ (see Fig. D.2).

Analogously to the above definition, we obtain the definition for $L_p(\Omega)$-spaces for $p \in [1, \infty)$.

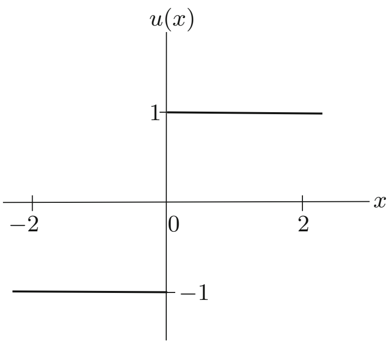

Fig. D.2 Function $u(x) = \mathrm{sgn}(x)$ in the interval (–2,2)

Definition D.3 $L_p(\Omega)$**-spaces**: Let Ω be a closed domain in $\mathbb{R}^n$. Then, the space of p-integrable functions is given by

$$L_p(\Omega) = \{u : \Omega \to \mathbb{R} | \int_{\Omega} |u(x)|^p \mathrm{d}x < \infty\} . \tag{D.6}$$

Let us assume that the function u has a continuous derivative u'. According to the formula for partial integration, we have for each continuously differentiable function φ with $\varphi(a) = \varphi(b) = 0$ the following relation

$$\int_a^b u(x)\varphi'(x)\,\mathrm{d}x = -\int_a^b u'(x)\varphi(x)\,\mathrm{d}x . \tag{D.7}$$

With the help of (D.7), we can define the derivative of functions, which have no finite derivative in the classical sense. If u and w denote integrable functions that fulfill the following relation

$$\int_a^b u(x)\varphi'(x)\,\mathrm{d}x = -\int_a^b w(x)\varphi(x)\,\mathrm{d}x \tag{D.8}$$

for all differentiable functions φ with $\varphi(a) = \varphi(b) = 0$, then the function w is called the *derivative* of u in the *weak sense* (with respect to x). The function u defined by (see Fig. D.3)

$$u(x) = \begin{cases} x+1 & \text{for} \quad -1 \le x \le 0 \\ 1-x & \text{for} \quad 0 < x \le 1 \end{cases}$$

will have no derivative in the classical sense at $x = 0$. Applying partial integration for differentiable functions $\varphi(x)$ with $\varphi(-1) = \varphi(1) = 0$, we obtain

$$\begin{aligned}
\int_{-1}^{1} u(x)\varphi'(x)\,\mathrm{d}x &= \int_{-1}^{0} (x+1)\varphi'(x)\,\mathrm{d}x + \int_{0}^{1} (1-x)\varphi'(x)\,\mathrm{d}x \\
&= -\int_{-1}^{0} \varphi(x)\,\mathrm{d}x + (x+1)\varphi(x)|_{-1}^{0} \\
&\quad -\int_{0}^{1} (-1)\varphi(x)\,\mathrm{d}x + (1-x)\varphi(x)\;|_{0}^{1} \\
&= -\left[\int_{-1}^{0} \varphi(x)\,\mathrm{d}x + \int_{0}^{1} (-1)\varphi(x)\,\mathrm{d}x\right] + \underbrace{\varphi(0) - \varphi(0)}_{=0} .
\end{aligned}$$

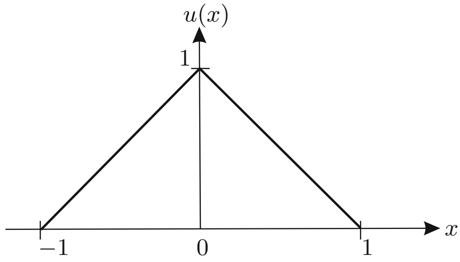

Fig. D.3 Example of a function in $H^1(a, b)$

Therefore, in the weak sense of differentiation we obtain

$$u'(x) = \begin{cases} 1 & \text{for} \quad -1 \leq x < 0 \\ -1 & \text{for} \quad 0 < x \leq 1 \end{cases}$$

with an arbitrary value for $u'(0)$.

Definition D.4 *Sobolev space*: Let Ω be a domain in $\mathbb{R}^n$. The functional space

$$W_p^m(\Omega) = \{u \in L_p(\Omega) | D^\alpha u \in L_p, |\alpha| \leq m\} \tag{D.9}$$

is called Sobolev space $W_p^m(\Omega)$. The partial derivatives of u are defined in the weak sense.

The appropriate norms on Sobolev spaces are defined by

$$||u||_{W_p^m(\Omega)} = \left(\int\limits_\Omega \sum_{|\alpha| \leq m} |D^\alpha u|^p \, \mathrm{d}x \right)^{1/p} \tag{D.10}$$

and its semi-norm by

$$|u|_{W_p^m(\Omega)} = \left(\int\limits_\Omega \sum_{|\alpha| = m} |D^\alpha u|^p \, \mathrm{d}x \right)^{1/p} . \tag{D.11}$$

If we restrict p to two, then we obtain a Hilbert space ($W_2^m(\Omega) = H^m(\Omega)$) with the scalar product

$$(u, v) = \int\limits_\Omega \left(\sum_{|\alpha| \leq m} D^\alpha u D^\alpha v \right) \mathrm{d}x \, . \tag{D.12}$$

For example, the function $u(x)$ is in the space $H^1(a,b)$, if $u'(x)$ exists and is within the space $L^2(a,b)$. The norm is computed via

$$||u||_{H^1(a,b)} = \sqrt{\int_a^b (u(x))^2 \,\mathrm{d}x + \int_a^b (u'(x))^2 \,\mathrm{d}x}\,, \tag{D.13}$$

its semi-norm by

$$|u|_{H^1(a,b)} = \sqrt{\int_a^b (u'(x))^2 \,\mathrm{d}x}\,, \tag{D.14}$$

and the scalar product as follows

$$(u,v)_{H^1(a,b)} = \int_a^b u(x)v(x)\,\mathrm{d}x + \int_a^b u'(x)v'(x)\,\mathrm{d}x\,. \tag{D.15}$$

Definition D.5 Let Ω be a domain in $\mathbb{R}^n$ and denote by $C_0^\infty(\Omega)$ the space of infinitely often differentiable functions with zero boundary values. Then we write for the closure of $C_0^\infty(\Omega)$ with respect to the H^1 norm

$$H_0^1(\Omega) = \overline{C_0^\infty(\Omega)}^{H^1(\Omega)} \subset H^1(\Omega)\,. \tag{D.16}$$

Definition D.6 *Partial Integration*: Let $\Omega \subset \mathbb{R}^n, n = 2, 3$ be a domain with smooth boundary Γ. Then, for any $u, v \in H^1(\Omega)$ the following relation holds

$$\int_\Omega \frac{\partial u}{\partial x_i} v \,\mathrm{d}x = \int_\Gamma u v\, \boldsymbol{n}\cdot\boldsymbol{e}_i \,\mathrm{d}s - \int_\Omega u \frac{\partial v}{\partial x_i}\,\mathrm{d}x\,. \tag{D.17}$$

In (D.17) n denotes the outer normal and $\bar{\Omega}$ the considered domain Ω with boundary Γ.

By a multiple application of (D.17), we arrive at **Green's formula**

$$\int_\Omega \Delta u\, v\,\mathrm{d}x = \int_\Gamma \frac{\partial u}{\partial n} v\,\mathrm{d}s - \int_\Omega (\nabla u)^T\, \nabla v\,\mathrm{d}x \tag{D.18}$$

for all $u \in H^2(\Omega)$ and $v \in H^1(\Omega)$.

Appendix E
Solution of Nonlinear Equations

In this section we are concerned with the solution of systems of nonlinear equations. As an example, we will consider the nonlinear Poisson equation, given as follows

$$-\nabla \cdot \varepsilon(|\nabla u|)\nabla u - f = 0 \tag{E.1}$$

$$u = 0 \quad \text{on } \Gamma\,. \tag{E.2}$$

This defines a nonlinear operator $\mathcal{F}$ that allows us to rewrite (E.1) and (E.2) as

$$\mathcal{F}(u) = 0\,. \tag{E.3}$$

The weak formulation of (E.1) and (E.2) for all test functions $v \in H_0^1$ reads as

$$\int_\Omega \varepsilon(|\nabla u|)\nabla v \cdot \nabla u \,\mathrm{d}\Omega - \int_\Omega v f \,\mathrm{d}\Omega = 0\,. \tag{E.4}$$

By applying the finite element method, we arrive at the following algebraic system

$$\boldsymbol{K}(\underline{u})\underline{u} = \underline{f}\,, \tag{E.5}$$

with the matrix $\boldsymbol{K} \in \mathbb{R}^{n\times n}$, $\underline{f} \in \mathbb{R}^n$, $\underline{u} \in \mathbb{R}^n$ and n the number of unknowns. Since we cannot solve (E.5) explicitly, we have to establish an approximate solution by setting up a series $\underline{u}_k$ ($k = 0, 1, 2, 3, ..$) that is supposed to converge to the correct solution. Concerning the rate of convergence, we will restrict the discussion to the following types:

Definition E.1 *Convergence*: Let $\underline{u}^* \in \mathbb{R}^n$ be the exact solution. Then

- $\underline{u}_k$ converges towards $\underline{u}^*$ *q-quadratically* (q stands for quotient), if there exists a C such that

$$||\underline{u}_{k+1} - \underline{u}^*|| \le C||\underline{u}_k - \underline{u}^*||^2\,. \tag{E.6}$$

M. Kaltenbacher, *Numerical Simulation of Mechatronic Sensors and Actuators*,
DOI 10.1007/978-3-642-40170-1

- $\underline{u}_k$ converges towards $\underline{u}^*$ *q-linearly* with the q-factor $\sigma \in (0, 1)$, if

$$||\underline{u}_{k+1} - \underline{u}^*|| \leq \sigma ||\underline{u}_k - \underline{u}^*|| \,. \tag{E.7}$$

In general, a *q-quadratically* convergent algorithm is preferable to a *q-linearly* convergent one. However, we always have to take into account the numerical cost for one iteration. Therefore, in some cases the method with the slower convergence rate can even be faster.

Since we solve (E.5) numerically by computing a series of approximating solutions $\underline{u}_k$, the question of the stopping criterion is of great importance. In general, we distinguish between the following two types of stopping criteria:

(1) **Error criterion**:
We take the solutions of two successive iteration steps and define an absolute accuracy ε^{abs} by

$$||\underline{u}_{k+1} - \underline{u}_k||_2 < \varepsilon^{\text{abs}} \,, \tag{E.8}$$

and a relative accuracy ε^{rel} by

$$||\underline{u}_{k+1} - \underline{u}_k||_2 < \varepsilon^{\text{rel}} ||\underline{u}_{k+1}||_2 \,, \tag{E.9}$$

which has to be achieved. However, in some analysis the true solution may still be far away, although the above-defined stopping criteria are fulfilled. This may particularly occur in the solution methods that have to use a line search (see Sect. E.1) to avoid possible divergence during early steps of the iteration process or due to nonmonotonic material relations. Then, it can happen that the control parameter becomes very small, which results in almost no difference between $\underline{u}_{k+1}$ and $\underline{u}_k$.

(2) **Residual criterion**:
By computing the residual of the obtained solution, we can define an absolute accuracy $\varepsilon_{\text{res}}^{\text{abs}}$ by

$$||\boldsymbol{K}(\underline{u}_{k+1})\underline{u}_{k+1} - \underline{f}||_2 < \varepsilon_{\text{res}}^{\text{abs}} \,, \tag{E.10}$$

as well as a relative accuracy $\varepsilon_{\text{res}}^{\text{rel}}$ by

$$||\boldsymbol{K}(\underline{u}_{k+1})\underline{u}_{k+1} - \underline{f}||_2 < \varepsilon_{\text{res}}^{\text{rel}} ||\underline{f}||_2 \,. \tag{E.11}$$

As shown in Fig. E.1, according to the problem type, this stopping criterion may also be reached too early.

As a consequence of the above discussion, it is preferable to check both stopping criteria.

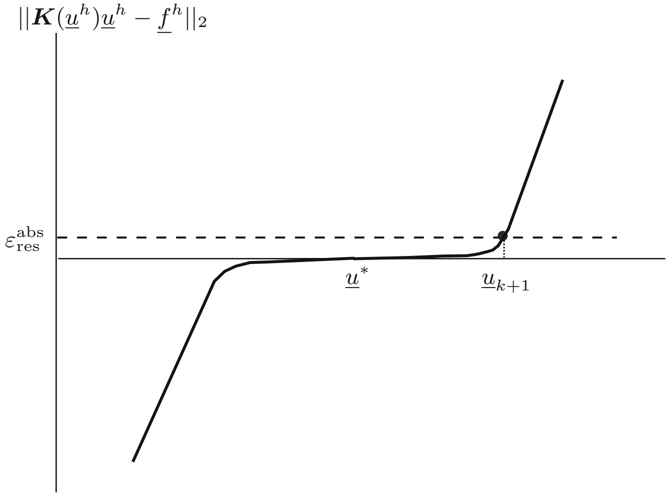

Fig. E.1 Obtained solution $\boldsymbol{u}_{k+1}$ is still far away from the true solution $\boldsymbol{u}^*$

E.1 Fixed-point Iteration

The simplest method of solving (E.5) is to rewrite it as a fixed-point equation

$$\underline{u} = \boldsymbol{K}^{-1}(\underline{u})\,\underline{f}\,. \tag{E.12}$$

This will result in the following sequence

$$\underline{u}_{k+1} = \boldsymbol{K}^{-1}(\underline{u}_k)\,\underline{f} \tag{E.13}$$

$$\boldsymbol{K}(\underline{u}_k)\underline{u}_{k+1} = \underline{f}\,. \tag{E.14}$$

Thus, we can write the damped fixed-point iteration method as follows

$$\boldsymbol{K}(\underline{u}_k)\Delta\underline{u} = \underline{f} - \boldsymbol{K}(\underline{u}_k)\underline{u}_k = \underline{r}(\underline{u}_k) \tag{E.15}$$

$$\underline{u}_{k+1} = \underline{u}_k + \eta\Delta\underline{u}\,. \tag{E.16}$$

The nodal vector $\underline{r}(\underline{u})$ is known as the residual of the problem and a solution is given by the set of nodal values $\underline{u}$, for which the residual is zero. The scalar parameter $\eta \in [0, 1]$ is introduced to control the possible divergence during the early steps of the iteration process or due to nonmonotonic material relations. A common algorithm to compute η is a *line search* (see [1]) defined by

$$|G(\eta)| \to \min\,, \tag{E.17}$$

with

$$G(\eta) = \Delta\underline{u} \cdot \underline{r}(\underline{u}_k + \eta\Delta\underline{u})\,. \tag{E.18}$$

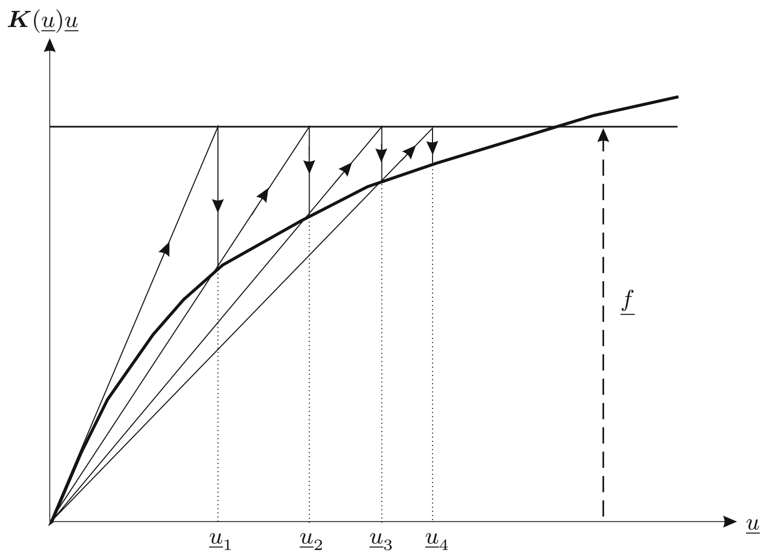

Fig. E.2 Graphical interpretation for solving a nonlinear equation using the fixed-point method

One simple method of approximating the optimal η is as follows

1. Evaluate $g_1 = G(0.1)$ and $g_2 = G(1.0)$
2. Calculate the straight line $l(g_1, g_2)$ between g_1 and g_2
3. Calculate the value $\eta = \frac{10g_1 - g_2}{10\cdot(g_2 - g_1)}$ for which $l(g_1, g_2) = 0$ holds

A graphical interpretation of the fixed-point method is given in Fig. E.2.

E.2 Newton's Method

Let us introduce the following linearization of the nonlinear operator $\mathcal{F}(u)$ at u_k

$$\mathcal{F}(u) \approx \mathcal{F}(u_k) + \mathcal{F}'(u_k)[s] \tag{E.19}$$

with $u_{k+1} = u_k + s$. The term $\mathcal{F}'(u_k)[s]$ denotes the *Frechét—derivative* of the nonlinear operator $\mathcal{F}$ at u_k in the direction of s and is defined as follows

Definition E.2 *Frechét—derivative*: Let $\boldsymbol{X}$ and $\boldsymbol{Y}$ be two normed vector spaces and $\boldsymbol{D} \subset \boldsymbol{X}$ an open domain. The operator $\mathcal{F} : \mathcal{D} \to \boldsymbol{Y}$ is differentiable in the sense of Frechét at x, iff there exists an operator $\boldsymbol{A} : \boldsymbol{X} \to \boldsymbol{Y}$, so that for all $y \in \boldsymbol{D}$

$$\mathcal{F}(y) = \mathcal{F}(x) + \boldsymbol{A}(y - x) + \boldsymbol{R}(x, y)\,,$$

with

$$\lim_{y\to x} \frac{||\boldsymbol{R}(x, y)||}{||y - x||} = 0$$

is fulfilled. $\boldsymbol{A}$ is the Frechét derivative $\mathcal{F}'(x)$.

Therefore, Newton's method reads as

$$\mathcal{F}'(u_k)[s] = -\mathcal{F}(u_k) \tag{E.20}$$

$$u_{k+1} = u_k + s\,. \tag{E.21}$$

Analogously to the fixed-point method, a line-search parameter may accelerate the convergence, and in addition may guarantee a global convergence of the Newton method. A graphical interpretation of Newton's method is displayed in Fig. E.3. To derive the Frechét derivative $\mathcal{F}'$ and Newton's method for the nonlinear Poisson equation given in (E.1), we first compute the difference between $\mathcal{F}(u+s)$ and $\mathcal{F}(u)$ in the weak formulation for arbitrary test functions $v \in H_0^1$

$$\int_\Omega \varepsilon(|\nabla(u+s)|)\nabla v \cdot \nabla(u+s)\,\mathrm{d}\Omega - \int_\Omega \varepsilon(|\nabla u|)\nabla v \cdot \nabla u\,\mathrm{d}\Omega\,. \tag{E.22}$$

Now, we will add to and at the same time subtract from (E.22) the term $\int_\Omega \varepsilon(|\nabla(u)|)$ $\nabla v \cdot \nabla(u+s)\,\mathrm{d}\Omega$, and obtain

$$\int_\Omega \left(\varepsilon(|\nabla(u+s)|) - \varepsilon(|\nabla u|)\right) \nabla v \cdot \nabla(u+s)\,\mathrm{d}\Omega + \int_\Omega \varepsilon(|\nabla u|)\nabla v \cdot \nabla s\,\mathrm{d}\Omega\,.$$

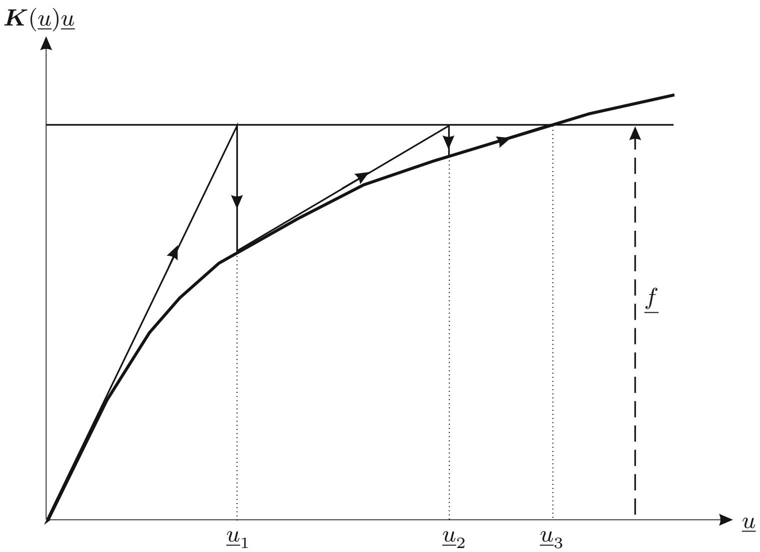

Fig. E.3 Graphical interpretation for solving a nonlinear equation using Newton's method

The term $\varepsilon(|\nabla(u+s)|) - \varepsilon(|\nabla u|)$ can be approximated as follows

$$\varepsilon(|\nabla(u+s)|) - \varepsilon(|\nabla u|) \approx \varepsilon'(|\nabla u|)\,(|\nabla(u+s)| - |\nabla u|)\ . \tag{E.23}$$

Now, let us investigate the term $(|\nabla(u+s)| - |\nabla u|)$

$$|\nabla(u+s)| - |\nabla u| = \frac{|\nabla(u+s)|^2 - |\nabla u|^2}{|\nabla(u+s)| + |\nabla u|} \tag{E.24}$$

$$= \frac{\nabla u\cdot\nabla u + \nabla s\cdot\nabla s + 2\nabla u\cdot\nabla s - \nabla u\cdot\nabla u}{|\nabla(u+s)| + |\nabla u|} \tag{E.25}$$

$$\approx \frac{\nabla u\cdot\nabla s}{|\nabla u|}\ . \tag{E.26}$$

With this result, we can write

$$\int_\Omega (\varepsilon(|\nabla(u+s)|) - \varepsilon(|\nabla u|))\,\nabla v\cdot\nabla(u+s)\,\mathrm{d}\Omega$$

$$\approx \int_\Omega \varepsilon'(|\nabla u|)\frac{\nabla u\cdot\nabla s}{|\nabla u|}\nabla v\cdot\nabla u\,\mathrm{d}\Omega\ . \tag{E.27}$$

Summarizing the above results, we conclude that the Frechét derivative $\mathcal{F}'(u_k)[s]$ in the weak formulation of the PDE for a test function v is given by

$$\int_\Omega \varepsilon(|\nabla u_k|)\nabla v\cdot\nabla s\,\mathrm{d}\Omega + \int_\Omega \varepsilon'(|\nabla u_k|)\frac{\nabla u_k\cdot\nabla s}{|\nabla u_k|}\nabla v\cdot\nabla u_k\,\mathrm{d}\Omega\ . \tag{E.28}$$

Therefore, by using (E.20) as well as (E.21), we obtain Newton's method for the nonlinear Poisson equation

$$\int_\Omega \varepsilon(|\nabla u_k|)\nabla v\cdot\nabla s\,\mathrm{d}\Omega + \int_\Omega \varepsilon'(|\nabla u_k|)\frac{\nabla u_k\cdot\nabla s}{|\nabla u_k|}\nabla v\cdot\nabla u_k\,\mathrm{d}\Omega$$

$$= \int vf\,\mathrm{d}\Omega$$

$$- \int_\Omega \varepsilon(|\nabla u_k|)\nabla v\cdot\nabla u_k\,\mathrm{d}\Omega \qquad \forall v\in H_0^1(\Omega)$$

$$u_{k+1} = u_k + s\ . \tag{E.29}$$

By apply the finite element method to the above equation, we will arrive at the appropriate algebraic system of equations.

Appendix F
Hysteresis Model

One of the most general hysteresis models used is named after F. Preisach, who developed it in 1935. Preisach's approach was purely intuitive and was based on plausible hypotheses concerning magnetic material behavior [2]. A mathematical-based investigation was performed by M. Krasnoselskii in the 1970s (see e.g., [3]).

In order to get some physical as well as mathematical understanding, let us investigate some properties of Preisach's hysteresis model. Thus, we consider an infinite set of elementary hysteresis operators $\mathcal{R}_{\beta,\alpha}$, where each of them can be represented by a rectangular loop (see Fig. F.1). Since we want to model the hysteresis within dielectric materials, we choose for the input quantity the normalized electric field intensity e and for the output quantity the normalized polarization p according to

$$e = \frac{E}{E_{\mathrm{sat}}} \qquad p = \frac{P}{P_{\mathrm{sat}}}\,. \tag{F.1}$$

In (F.1) E_{sat} denotes the saturated electric field intensity and P_{sat} the saturated electric polarization. In Fig. F.1 α and β are the up and down switching values and according to these switching values, the input will lead to an output value $+1$ or -1. Restricting the switching values to $\alpha \geq \beta$ and $|\alpha|, |\beta| \leq 1$ leads to the following set S (see Fig. F.2)

$$(\alpha, \beta) \in S \quad \text{with } S = \{(\alpha, \beta) \in \mathbb{R}^2, |\alpha|, |\beta| \leq 1, \beta \leq \alpha\}\,. \tag{F.2}$$

Therewith, we describe the class of hysteresis loops with closed major loop [4]. Now, the Preisach operator for the electric polarization p computes as

$$p(t) = \int_S \wp(\alpha, \beta)\mathcal{R}_{\beta,\alpha}(e(t))\, d\alpha d\beta\,. \tag{F.3}$$

M. Kaltenbacher, *Numerical Simulation of Mechatronic Sensors and Actuators*,
DOI 10.1007/978-3-642-40170-1

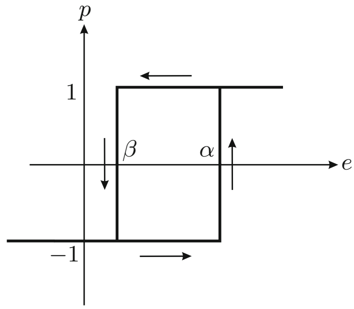

Fig. F.1 Rectangular hysteresis loop

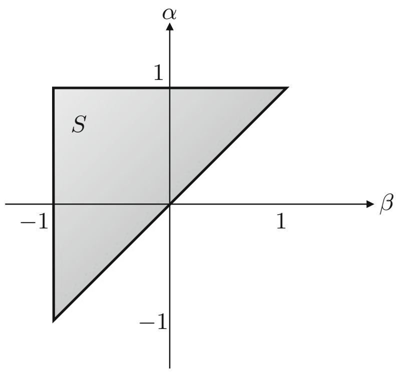

Fig. F.2 Set S for possible switching values α and β

In (F.3) $\wp$ denotes the Preisach function, which defines the shape of the hysteresis loops and fulfills the following properties [4]

$$\wp(\alpha, \beta) \quad \begin{Bmatrix} \geq 0 & \text{for } (\alpha, \beta) \in S \\ = 0 & \text{for } (\alpha, \beta) \notin S \end{Bmatrix} \tag{F.4}$$

$$\int_S \wp(\alpha, \beta)\, d\alpha d\beta = 1 \tag{F.5}$$

$$\wp(-\beta, -\alpha) = \wp(\alpha, \beta)\,. \tag{F.6}$$

Now let us assume that the input $e(t)$ increases monotonically up to a value of e_1 at $t = t_1$. Thus, all $\mathcal{R}_{\beta,\alpha}$ operators with α less than e_1 switch up, which means that their outputs take on the value of $+1$. Within the set S of possible (α, β) values, we will obtain a straight line parallel to the β-axis with $\alpha = e_1$ (see Fig. F.3a). In the next step, we assume that the input $e(t)$ starts to decrease monotonically to a value of e_2 at t_2. Now, all $\mathcal{R}_{\beta,\alpha}$ operators with down-switching values β larger than e_2 will turn back, so that their output takes on the value of -1. This leads to a straight line parallel to the α-axis with value $\beta = e_2$, which is illustrated in Fig. F.3a. Therefore, as illustrated in Fig. F.3a, we can subdivide the region S into S^+ (p takes on the value of $+1$) and S^- (p takes on the value of -1). For the general case, a staircase line

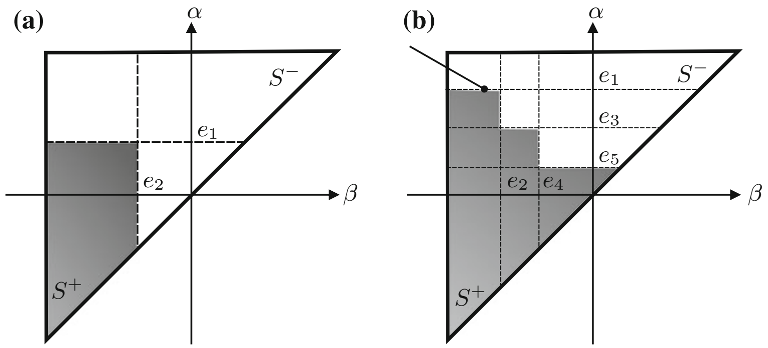

Fig. F.3 Decomposing into S^+ and S^-. **a** $e(t)$ increases till e_1 and decreases till e_2, **b** Staircase line $L(t)$

$L(t)$ will subdivide S into S^+ and S^- (see Fig. F.3b) according to the following two rules:

- A monotonically increasing input signal $e(t)$ defines a straight line parallel to the β-axis with value $e(t)$.
- A monotonically decreasing input signal $e(t)$ defines a straight line parallel to the α-axis with value $e(t)$.

Therefore, the horizontal lines represent relative maxima and the vertical lines relative minima. In addition, by storing the local maxima and minima, the hysteresis can be uniquely constructed.

Due to the *wiping-out* property, not all relative maxima and minima have to be stored. This property states that each local input maximum wipes out the vertical $L(t)$ whose α values are below this maximum, and each local minimum wipes out the vertices whose β values are above the minimum [4]. The wiping out is best illustrated by an input signal $e(t)$ as displayed in Fig. F.4. Only the relative maxima e_1 and e_3

Fig. F.4 Input signal $e(t)$ for illustration of the wiping out property

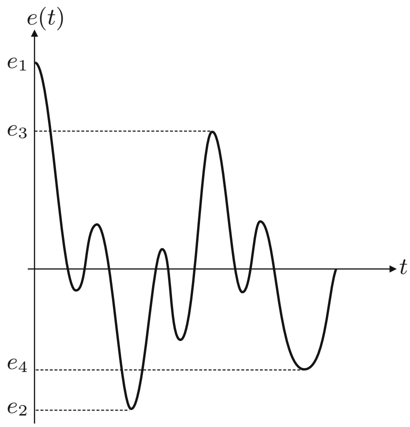

as well as relative minima e_2 and e_4 have to be stored. All other maxima (minima) will be intermediately stored during the process in a list, but will be deleted due to the wiping-out property.

Furthermore, the Preisach model fulfills the *congruence* property [4], which states that all minor hysteresis loops corresponding to back-and-forth variations of inputs between the same two consecutive extrema are congruent (see Fig. F.5).

For the numerical computation of the Preisach operator, the following efficient evaluation has been developed. With e_1, ..., e_n those relative input extrema that have not been wiped out yet at time t, the value of the output at time t computes as

$$p(t) = \mathcal{E}(-e_1, e_1) + 2\sum_{i=1}^{n-1} \mathcal{E}(e_i, e_{i+1}), \tag{F.7}$$

with $\mathcal{E}(e_i, e_{i+1})$ the *Everett* function (see Fig. F.6)

$$\mathcal{E}(e_1, e_2) = \int\limits_{T(e_1,e_2)} \wp(\alpha, \beta)\, d\alpha d\beta\,. \tag{F.8}$$

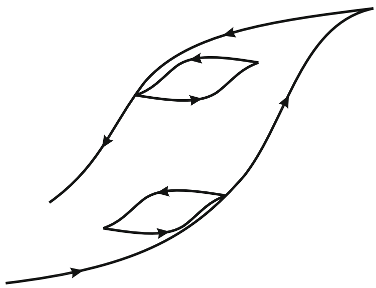

Fig. F.5 Congruency property of the hysteresis model

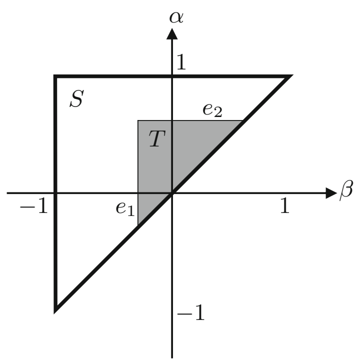

Fig. F.6 Computation of the Everett function $\mathcal{E}(e_1, e_2)$

For the simplest Preisach function $\wp(\alpha, \beta) = 1/2$, the Everett function computes as

$$\mathcal{E}(e_1, e_2) = \frac{1}{4}(e_2 - e_1)^2 \operatorname{sgn}(e_2 - e_1)\,. \tag{F.9}$$

Thus, we have an efficient model for taking into account ferroelectric hysteresis within piezoelectric materials. For a detailed discussion concerning hysteresis operators in PDEs, and especially their identification from measured data, we refer to [5].

References

1. O.C. Zienkiewicz and R.L. Taylor, The Finite Element Method, vol. 2, Butterworth - Heinemann, 2003.
2. E. Preisach, über die magnetische Nachwirkung, Z. Phys. (1935), no. 94, 277–302.
3. M. Krasnoselskii, A. Pokrovskii, *Systems with Hysteresis* (Nauka, Tech. report, 1983)
4. I.D. Mayergoyz, *Mathematical Models of Hysteresis* (Springer Verlag, New York, 1991)
5. B. Kaltenbacher, M. Kaltenbacher, *Modelling and iterative identification of hysteresis via Preisach operators in PDEs* (Radon Series Comp. Appl, Math, 2007)

Index

M. Kaltenbacher, *Numerical Simulation of Mechatronic Sensors and Actuators*,
DOI 10.1007/978-3-642-40170-1